$O_2(a^1\Delta_g)$ Absorption and $O_2(b^1\Sigma_g^+)$ Emission in Solution: Quantifying the a−b Stokes Shift†

Tamás Keszthelyi, Tina D. Poulsen, and Peter R. Ogilby*

Department of Chemistry, Aarhus University, Langelandsgade 140, DK-8000 Århus C, Denmark

Kurt V. Mikkelsen*

Department of Chemistry, H. C. Ørsted Institute, University of Copenhagen, DK-2100 Copenhagen Ø, Denmark

Received: March 28, 2000; In Final Form: August 8, 2000

In a nanosecond time-resolved infrared spectroscopic study of dissolved oxygen, $O_2(a^1\Delta_g)$ absorption, i.e., $a^1\Delta_g \rightarrow b^1\Sigma_g^+$, and $O_2(b^1\Sigma_g^+)$ emission, i.e., $b^1\Sigma_g^+ \rightarrow a^1\Delta_g$, were monitored at ∼5200 cm^{-1} in a number of solvents. The maxima of the respective spectra depend significantly on the solvent, indicating that the $O_2(a^1\Delta_g)$ and $O_2(b^1\Sigma_g^+)$ energy levels likewise depend significantly on the solvent. The corresponding Stokes shifts, however, are small. The latter, recorded as the difference between the absorption and emission maxima, do not exceed the uncertainty limits that derive from the step-scan Fourier transform spectroscopic measurements (∼ ±3 cm^{-1}). Nevertheless, the data clearly indicate that the difference between the equilibrium and nonequilibrium solvation energies for the $O_2(a^1\Delta_g)$ and $O_2(b^1\Sigma_g^+)$ states is not large. Within the error limits, it is not possible to ascertain if the Stokes shifts are solvent dependent. Ab initio computational methods were used to model the data, and the results indicate that both long- and short-range interactions between oxygen and the perturbing solvent must be considered to adequately describe spectroscopic transitions in dissolved oxygen. The computational results indicate that a 1:1 complex between oxygen and the perturbing molecule embedded in a dielectric continuum appears to provide a sufficiently accurate model that can be used to probe subtle solvent−oxygen interactions.

Introduction

The effect of solvent on the radiative transitions of dissolved oxygen continues to provide pertinent and challenging problems for study.[1,2] The lowest excited electronic state of oxygen, $O_2(a^1\Delta_g)$, is an acknowledged reactive intermediate in many processes.[3,4] Thus, for experiments in which $O_2(a^1\Delta_g)$ is spectroscopically monitored, a solvent effect on the radiative transition can have important ramifications. From a more fundamental perspective, studies of solvent effects on radiative transitions provide a nice way to investigate mechanisms by which a host medium can perturb a dissolved solute. Oxygen is particularly interesting in this regard simply because transitions between $O_2(a^1\Delta_g)$ and both the ground state $[O_2(X^3\Sigma_g^-)]$ and second excited state $[O_2(b^1\Sigma_g^+)]$ are formally forbidden as electric dipole processes. Moreover, many oxygen−solvent model systems are small enough to be amenable to high-level computational treatment which, in turn, facilitates the interplay between theory and experiment.

Accurate a → X phosphorescence spectra have been obtained from a wide range of common solvents upon irradiation of a singlet oxygen sensitizer at atmospheric pressure.[5,6] Unfortunately, to record X → a absorption spectra requires the use of comparatively long path lengths (∼1−5 cm) and high oxygen pressures (∼140 atm).[7−10] Furthermore, because of the dangers of combustion, such high pressure experiments can only be performed in a limited number of solvents. Thus, it is difficult to probe details of the a−X transition using complementary absorption and emission experiments.

We have recently shown that, using a step-scan Fourier transform (FT) infrared spectrometer, the a → b absorption spectrum at ∼5200 cm^{-1} can be recorded in nanosecond time-resolved experiments.[11,12] In this approach, $O_2(a^1\Delta_g)$ is produced via pulsed-laser irradiation of a sensitizer. Most importantly, the data are obtained from common solvents at atmospheric pressure using path lengths that can be as short as ∼100 μm. It is likewise possible to record the b → a fluorescence spectrum, again upon pulsed-laser irradiation of a sensitizer, using either a step-scan FTIR spectrometer[12] or a dispersion-based instrument.[13,14] Thus, complementary emission and absorption data from the b−a transition can be used to monitor subtle effects of solvent on dissolved oxygen.

We have also recently shown that ab initio computational methods can be used to obtain energies and properties (e.g., polarizabilities) of dissolved oxygen under both equilibrium and nonequilibrium solvation conditions.[15−17] Most of this work, however, focused on the a → X transition. To complement b−a experimental studies, therefore, it will be necessary to extend our theoretical effort to include more work on $O_2(b^1\Sigma_g^+)$.

In this current paper, we present results from a combined experimental and theoretical study of the a−b transition in dissolved oxygen. The key components of this study are illustrated in Scheme 1.

Specifically, for a → b absorption, we consider a transition from $O_2(a^1\Delta_g)$ in equilibrium with the surrounding solvent to the nonequilibrated $O_2(b^1\Sigma_g^+)$ Franck−Condon state. For b → a emission, we consider a transition from solvent-equilibrated $O_2(b^1\Sigma_g^+)$ to the nonequilibrated $O_2(a^1\Delta_g)$ Franck−Condon state. The Stokes shift, therefore, recorded as the difference between the absorption and emission maxima, is a

† Part of the special issue "C. Bradley Moore Festschrift".
* To whom correspondence should be addressed.

10.1021/jp0011692 CCC: $19.00
Published on Web 10/05/2000

SCHEME 1

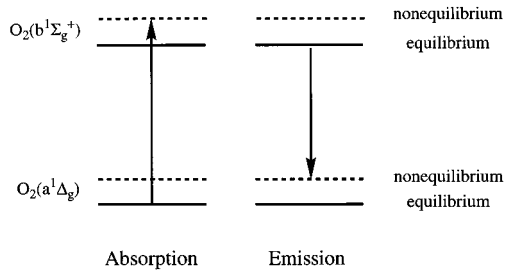

measure of the difference between the equilibrium and nonequilibrium solvation energies for both the $O_2(a^1\Delta_g)$ and $O_2(b^1\Sigma_g^+)$ states. On the basis of an earlier b → a emission study,[14] we ascertained that b−a transition energies are indeed sensitive to the solvent. For the present study, we set out to examine the extent to which the a−b Stokes shift is solvent dependent.

Experimental and Computational Methods

Details of the experimental approach to record time-resolved b → a emission and a → b absorption spectra at ∼5200 cm^{-1} are given elsewhere.[12] In all cases, both the $O_2(b^1\Sigma_g^+)$ and $O_2(a^1\Delta_g)$ states of oxygen were created upon pulsed-laser irradiation of a singlet oxygen photosensitizer. The laser (Quanta-Ray GCR 230 Nd:YAG) was operated at a 10 Hz repetition rate, and the irradiation wavelength was tuned throughout the UV/vis region using (1) the second, third, and fourth harmonics of the Nd:YAG fundamental output, (2) an optical parametric oscillator whose output could also be doubled, and/or (3) a high-pressure cell of H_2 gas as a Raman shifting medium. Data were obtained using a modified Bruker model IFS-66v/s step-scan FT spectrometer equipped with a 77 K InSb detector. Spectrometer modifications included (1) incorporation of an external power supply for the detector and detector preamplifier, (2) changes in the preamplifier that made it easier to acquire both ac- and dc-coupled signals, and (3) more rigorous electronic shielding and grounding. Signals were digitized with either a 40 MHz, 12-bit (a → b absorption) or 200 MHz, 8-bit (b → a emission) analog-to-digital converter. The wavenumber scale automatically established by the FTIR with an internal laser was verified using known spectral transitions in water vapor at ∼5200 cm^{-1}.[18]

When monitoring $O_2(b^1\Sigma_g^+)$ fluorescence, the FT spectrometer's IR source was turned off. The sample was mounted outside the spectrometer and, after irradiation of the sensitizer, the b → a emission was collimated and coupled into the interferometer along the same optical axis ordinarily used by the IR source. Steps were taken to ensure that the sample volume from which light was emitted was correctly positioned at the FTIR collection port, thus minimizing errors in the wavenumber scale due to an incorrectly collimated source.[19] In particular, we established that when the fundamental output of a Nd:YVO_4-seeded Nd:YAG laser was scattered from a sample cuvette containing solvent, the wavenumber recorded by the FTIR, 9394 cm^{-1}, correctly fell in the expected range of 9393−9397 cm^{-1}.[20] Moreover, the value recorded varied only over a range of 2 cm^{-1} upon translation of the cuvette away from the optical axis of the collecting lens. Furthermore, the b → a emission maxima obtained with the FTIR were identical to those independently obtained using a grating monochromator.[14] With these data, we estimate that the b → a emission maxima recorded by the FTIR at ∼5200 cm^{-1} are accurate to within ∼2 cm^{-1}. Independent data from a → X emission spectra likewise recorded using FTIR spectrometers indicate that this ∼2 cm^{-1} accuracy estimate is indeed reasonable. Specifically, in experiments performed by two separate groups where accuracy errors associated with beam divergence in the FT spectrometer could likewise be a problem, the a → X emission maxima recorded were generally consistent to within ∼1−2 cm^{-1}.[5,6]

When monitoring $O_2(a^1\Delta_g)$ absorption, the sample was mounted between the interferometer and the detector in the spectrometer chamber designated for this purpose. A tungsten lamp was used as the IR source. The excitation laser was brought into the sample chamber through windows mounted in the spectrometer wall and coupled into the sample using prisms.

In both the $O_2(a^1\Delta_g)$ absorption and $O_2(b^1\Sigma_g^+)$ emission experiments, we could reproduce the band maxima recorded with a precision of ∼ ±1 cm^{-1}. For each solvent studied, this was established with a minimum of six separate measurements but, in some cases, involved as many as 15 measurements.

For most experiments, the sensitizer used was 9-fluorenone (Aldrich), which, depending on the experiment and the solvent, was irradiated at a wavelength in the range 290−450 nm. Perinaphthenone (Aldrich) was used as the sensitizer for the experiments in methanol. With the exception of the a → b absorption spectrum in methanol, all data were recorded using 1 cm path length cuvettes. The methanol data were recorded using a 0.1 cm path length cuvette due to significant absorption by the solvent itself at ∼5200 cm^{-1}. All experiments were performed in oxygen-saturated solutions at atmospheric pressure. Solvents were obtained from Aldrich (Spectrophotometric or HPLC grade) and were used as received.

Details of the computational approach used to model solvated oxygen are likewise given elsewhere.[15,16] Briefly, dielectric models generalized to include nonequilibrium as well as equilibrium solvation were used.[21−23] All calculations were performed with the DALTON program package.[24] Since molecular oxygen is an open-shell system, it is not advisable to use correlated methods based on a single determinant reference wave function. Instead, we used the multiconfigurational self-consistent field, MCSCF, approach. For work in which an "isolated" oxygen molecule was surrounded by a homogeneous dielectric medium (i.e., the continuum model), the calculations were performed with the aug-cc-pVQZ basis set. For work in which a complex between oxygen and a given solvent molecule (M) was embedded in a dielectric medium (i.e., the semicontinuum model), the aug-cc-pVDZ basis set was used.

Response theory[25,26] was used to calculate the transition energies. An attribute of response theory is the possibility to obtain many molecular properties in one single calculation.[27] In the spectral representation, response functions contain summations over all intermediate states. By employing response theory, however, any explicit reference to excited states is avoided, and the response equations are solved as sets of linear response equations using iterative techniques and direct linear transformations. The linear response function can be written as[27]

$$\langle\langle V^{\omega_0};V^{\omega_1}\rangle\rangle_{\omega_1} = P(0,1)\sum_n \frac{\langle 0|V^{\omega_0}|n\rangle\langle n|V^{\omega_1}|0\rangle}{\omega_1 - \omega_n} \qquad (1)$$

Since the a−b transition is formally forbidden as an electric dipole process but allowed as an electric quadrupole process, we let V^{ω_0} and V^{ω_1} refer to the electric quadrupole operator. Admittedly, for an M−O_2 complex, the a−b transition will acquire electric dipole character and one could arguably also use an electric dipole operator.[28] However, only the transition

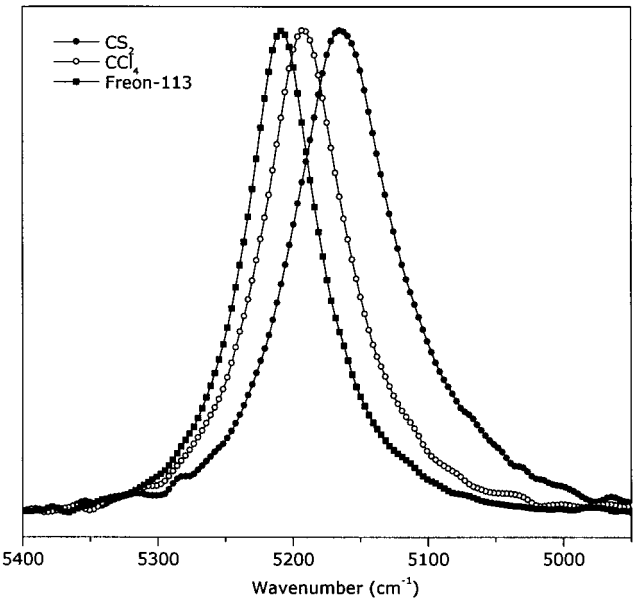

Figure 1. b → a Fluorescence spectra recorded in CS_2, CCl_4, and Freon-113. The data have been scaled such as to yield the same intensity at the emission maximum. The symbols shown on each spectrum are markers placed at intervals of ~3 cm^{-1}.

TABLE 1: Effect of Solvent on $O_2(a^1\Delta_g) \rightarrow O_2(b^1\Sigma_g^+)$ Absorption and $O_2(b^1\Sigma_g^+) \rightarrow O_2(a^1\Delta_g)$ Emission Maxima

solvent	solvent refractive index	a−b absorption maximum[a] (cm^{-1})	b−a emission maximum[a] (cm^{-1})	Stokes shift (cm^{-1})
CS_2	1.627	5168	5165	3
polystyrene glass	1.600	5184[b]		
toluene	1.496	5191		
CCl_4	1.460	5195	5192	3
n-hexane	1.375	5199		
Freon-113	1.358	5209	5208	1
methanol	1.329	5217		

[a] Error of ~±1 cm^{-1} on absorption data and ~±2 cm^{-1} on emission data. See Experimental Section for a detailed discussion of errors. [b] From Andersen and Ogilby.[37]

probabilities vary according to the operator used in the computations; the desired quantity for this study, the a−b transition energy, is independent of whether a dipole or quadrupole operator is used.

The a → b and b → a transition energies were obtained from the residues of the linear response functions, and the Stokes shift was obtained as the difference between these two numbers. Calculations on the $M-O_2(a^1\Delta_g)$ and $M-O_2(b^1\Sigma_g^+)$ complexes are more difficult due to the reduced symmetry of the system.[29] Under these circumstances, and given (1) the way the complete active space is allocated for a particular $M-O_2$ pair and (2) the flexibility of the specific basis set employed, the a → b and b → a transition energies computed can contain common and systematic errors. However, in taking the difference between these computed transition energies to yield the Stokes shift, these systematic errors cancel.

Results and Discussion

1. Experimental Data. *b−a Fluorescence.* $O_2(b^1\Sigma_g^+)$ fluorescence spectra (Figure 1) were recorded in three solvents; CS_2, CCl_4, and Freon-113 (1,1,2-trichlorotrifluoroethane). The emission maxima of the respective bands (Table 1) are consistent with those we reported in an earlier study using a dispersion-based spectrometer.[14]

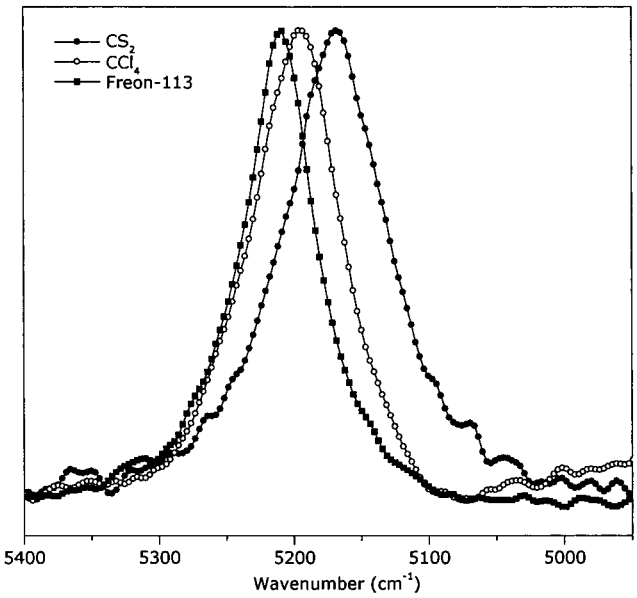

Figure 2. a → b Absorption spectra recorded in CS_2, CCl_4, and Freon-113. The data have been scaled such as to yield the same value at the absorption maximum. For each spectrum, absorbance values at the peak maximum are in the range 5×10^{-4} to 2×10^{-3}. The symbols shown on each spectrum are markers placed at intervals of ~3 cm^{-1}.

In using these three solvents, we demonstrate that the peak of the b → a emission spectrum depends significantly on the medium in which oxygen is dissolved. Results of earlier studies indicate that b → a spectral shifts correlate reasonably well with the solvent refractive index, *n*, as well as functions of *n* that represent, for example, the solvent electronic polarizability.[1,14,16] Specifically, the emission maximum shifts to a smaller wavenumber (i.e., a red shift) as *n* increases. The solvents chosen for study here cover a reasonably large range of *n* and thus likewise represent a comparatively large solvent-induced spectral shift. Unfortunately, it is difficult to record b → a emission spectra in a wide variety of neat solvents, specifically those with C−H and O−H bonds. In the latter solvents, nonradiative deactivation of $O_2(b^1\Sigma_g^+)$ is sufficiently facile as to (1) make the b → a fluorescence quantum yield very small and (2) render even the fastest IR detectors ineffective because of the short $O_2(b^1\Sigma_g^+)$ lifetime.[17,30]

a−b Absorption. $O_2(a^1\Delta_g)$ absorption spectra were likewise recorded in CS_2, CCl_4, and Freon-113 (Figure 2). The band maxima obtained from these spectra are also shown in Table 1.

Unlike b → a fluorescence, it is possible to record a → b absorption spectra in a wider variety of solvents, including those that contain C−H and O−H bonds. Absorption band maxima we have obtained from such solvents are also listed in Table 1. Using all of the a → b absorption data thus far available, we show in Figure 3 that the wavenumber of the band maximum correlates reasonably well with the refractive index, *n*, of the solvent in which oxygen is dissolved. This empirical relation is consistent with solvent effects observed on both the b → a and a → X emission maxima.[5,6,14] As explained in one of our earlier reports, however, caution must be exercised in ascribing physical meaning to this correlation.[16]

It is also important to note at this juncture that the width of both the a → b absorption as well as b → a emission bands varies with the solvent. Although this point has briefly been discussed in our earlier reports,[12,14] a more detailed treatment that exceeds the scope of the present paper is needed.

Stokes Shifts. The a−b Stokes shifts, recorded as the difference between the absorption and emission maxima, are

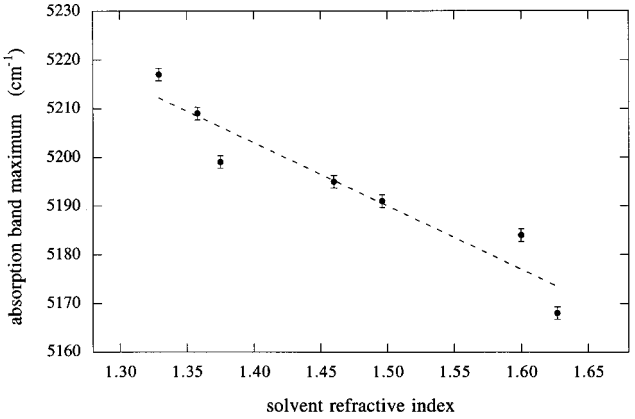

Figure 3. Plot of the a → b absorbance maximum against the refractive index, *n*, of the solvent in which oxygen is dissolved. Data used for this plot are listed in Table 1. The dashed line is a linear fit to the data.

not large and do not exceed the accuracy limits of the FT spectroscopic measurements (Table 1). These small Stokes shifts are further illustrated in Figure 4, where we superimpose corresponding absorption and emission spectra for each solvent studied. Although the absolute uncertainty of $\sim \pm 3$ cm^{-1} associated with the difference between the absorption and emission maxima exceeds the Stokes shifts reported, we nevertheless consistently record an emission spectrum that is slightly red-shifted with respect to the absorption spectrum (Figure 4). In earlier publications, we reported that the a−b Stokes shift in CS_2 was $\sim$10 cm^{-1}.[1,11,12] Although this shift is still quite small, this early determination appears to have been adversely influenced by a number of experimental factors associated with the use of a FTIR to detect emission [e.g., sample position and optics at collection port (see Experimental Section)]. A more accurate value for the a−b Stokes shift in CS_2 is the $\sim$3 cm^{-1} reported herein.

It is clear from Table 1 and Figures 1−3 that the maxima of the b → a emission and a → b absorption bands depend significantly on the solvent. Given the accuracy of our measurements, it is difficult to ascertain if the Stokes shifts likewise depend on solvent. Nevertheless, it is clear that, because the Stokes shifts are so small, any solvent-dependent change in the Stokes shift will likewise be small.

As indicated in the Introduction, it is difficult to probe the effect of solvent on the a−X transition using complementary absorption and emission experiments. The principal limitation is the need for high oxygen pressures to record X → a absorption spectra,[7−10] and to our knowledge, corresponding a → X emission spectra have not been recorded under similar high-pressure conditions. Because the a−X transition is sensitive to solvent perturbation,[1] there is sufficient reason to be cautious about comparing a → X emission maxima obtained at 1 atm to X → a absorption maxima obtained at pressures of $\sim$100 atm. With this caveat in mind, it is nevertheless interesting to note that Losev et al.[10] report data that yield solvent-dependent a−X Stokes shifts that range from 18 to 37 cm^{-1}. In light of our a−b data, the a−X data imply that the difference between the equilibrium and nonequilibrium solvation energies for the $O_2(a^1\Delta_g)$ and $O_2(X^3\Sigma_g^-)$ states is much larger than this same difference for the $O_2(a^1\Delta_g)$ and $O_2(b^1\Sigma_g^+)$ states. In turn, because the $O_2(a^1\Delta_g)$ state is common to both of these transitions, this implies that the difference between the equilibrium and non-equilibrium solvation energies of the $O_2(X^3\Sigma_g^-)$ state is much larger than that of the $O_2(a^1\Delta_g)$ and $O_2(b^1\Sigma_g^+)$ states. Thus, when data from a given solvent are compared to data recorded in the gas phase, for example, one might expect a larger shift in the

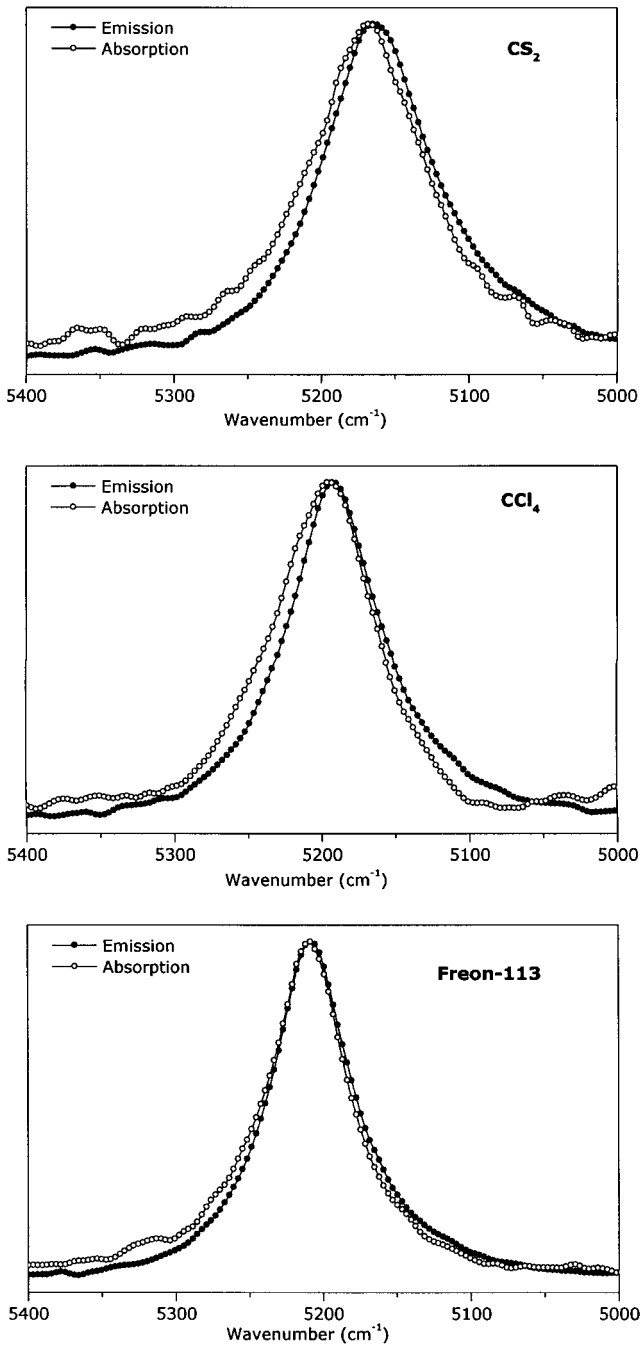

Figure 4. a−b absorption and emission spectra for a given solvent superimposed to illustrate the magnitude of the Stokes shift. The symbols shown on each spectrum are markers placed at intervals of $\sim$3 cm^{-1}.

a → X emission maximum than in the b → a emission maximum. This line of reasoning based on Losev's data, however, is not consistent with the available experimental data on b → a and a → X spectral shifts.[14] It thus appears that, given the magnitude of these subtle effects on dissolved oxygen, one must indeed be cautious when comparing data recorded at high oxygen pressures to data recorded at low oxygen pressures.

2. Computational Results. Two general approaches were used in this study to model the effect of solvent on dissolved oxygen. In the first, the continuum model, we enclosed oxygen in a spherical cavity surrounded by a homogeneous dielectric medium characterized by the macroscopic static and optical dielectric constants, ϵ_{st} and ϵ_{op}, respectively ($\epsilon_{op} = n^2$, where *n* is the solvent refractive index).[16] In the second, the semi-

continuum model, we formed a complex between oxygen and a given solvent molecule, M, and then embedded this $M-O_2$ complex in the dielectric medium, again characterized by ϵ_{st} and ϵ_{op}.[16]

In both models, the total polarization, $\mathbf{P}(\mathbf{r})$, is the sum of two contributions[25,26,31−35]

$$\mathbf{P}(\mathbf{r}) = \mathbf{P}_{op}(\mathbf{r}) + \mathbf{P}_{in}(\mathbf{r}) \quad (2)$$

The optical polarization, $\mathbf{P}_{op}$, represents the response from the solvent electronic degrees of freedom. Because of its very short relaxation time, $\mathbf{P}_{op}$ is assumed to always be in equilibrium with the charge distribution of the solute. The inertial polarization, $\mathbf{P}_{in}$, represents the response from the solvent nuclear degrees of freedom (i.e., vibrational, rotational, and translational motion) and remains fixed during an electronic transition, thus giving rise to a condition of nonequilibrium solvation. The condition of nonequilibrium solvation, the Franck−Condon state, will remain until inertial polarization moments can react to the change in the solute charge distribution engendered by the electronic transition. For the present work, it is important to recognize that both $O_2(a^1\Delta_g)$ and $O_2(b^1\Sigma_g^+)$ are sufficiently long-lived that the a → b and b → a transitions originate from solvent equilibrated states.

Continuum Model. In an earlier study, we established that the continuum approach does not accurately model a → X transition energies.[16] This conclusion is consistent with results obtained from computational work on other systems.[36] In the present study on the a−b transition, we likewise find that the continuum approach cannot model the experimental data. Specifically, calculated Stokes shifts fall in the range ∼5−70 cm^{-1}. As established in our earlier study,[16] a key weak point of the continuum model is that it fails to account for short-range interactions between oxygen and the perturbing solvent. We demonstrated that for the a → X transition, this deficiency can be overcome by using the semicontinuum model.[16]

Semicontinuum Model. In this approach, we consider a 1:1 complex between a given solvent molecule, M, and oxygen, $M-O_2$, that is embedded in a dielectric continuum. On the basis of our previous a → X computations, it is expected that this approach is sufficient to account for both short- as well as long-range interactions between oxygen and the perturbing solvent.

Calculations were performed for CS_2, CCl_4, and Freon-113. For each system, we considered a number of different orientations between M and O_2. For example, in Figure 5 we illustrate two of the orientations used for the Freon$-O_2$ complex. The $M-O_2$ orientations used for CS_2 and CCl_4 are illustrated elsewhere.[16] As expected, and as demonstrated with our earlier a → X computations,[16] the a−b transition energies depend on the relative M and O_2 orientations. Thus, the computed a−b Stokes shifts likewise vary with the orientation between M and O_2 (Table 2). To obtain an average of these computed Stokes shifts that accurately represents the experimental data, one should ideally consider a large sampling of M and O_2 orientations. Because energy differences between one $M-O_2$ orientation and another are small (i.e., the $M-O_2$ potential surfaces are shallow), appropriate weighting factors are the a−b transition probabilities associated with a particular $M-O_2$ orientation.[16] In the absence of these more extensive and demanding computations, it is nevertheless clear that the a−b Stokes shifts obtained for the limited number of $M-O_2$ orientations examined compare reasonably well with the experimental data (Table 2).

Conclusions

The maxima of the a → b and b → a spectra depend significantly on the solvent in which oxygen is dissolved. This indicates that the $O_2(a^1\Delta_g)$ and $O_2(b^1\Sigma_g^+)$ energy levels likewise depend significantly on the solvent. On the other hand, we find that the Stokes shifts for the a−b transition are comparatively small (<5 cm^{-1}). This observation indicates that the difference between the equilibrium and nonequilibrium solvation energies for the $O_2(a^1\Delta_g)$ and $O_2(b^1\Sigma_g^+)$ states is small. Because the Stokes shifts are so small, any solvent-dependent change in the Stokes shift will likewise be small. To accurately model the experimental data, one must consider both long- and short-range interactions between oxygen and the perturbing solvent. We have demonstrated that, to account for short-range interactions, it appears sufficient to consider a 1:1 complex between the perturbing solvent molecule and oxygen. Long-range interactions can be accommodated by using a dielectric continuum.

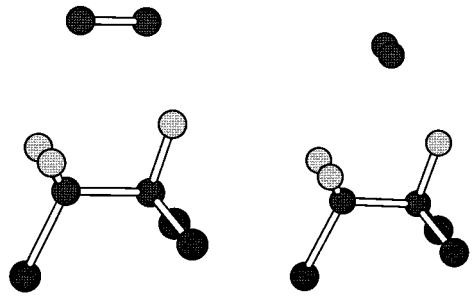

Figure 5. Structures that illustrate two of the orientations used in the Freon$-O_2$ computations. In both orientations shown, the Freon conformers have all of the fluorines on one face of the molecule, and we have brought oxygen down onto this face. The ease of the computations is greatly simplified if the complex has a plane of symmetry, and this is reflected in these $M-O_2$ orientations shown. The distance between M and O_2 is a variable that is altered in the computations. The orientation in which the oxygen internuclear axis is parallel to the Freon C−C axis yields a Stokes shift of 14 cm^{-1}, whereas the orientation in which the internuclear axes are perpendicular yields a Stokes shift of 0.2 cm^{-1}. Analogous results were also obtained for computations performed with oxygen on the chlorine face of the Freon (Table 2).

TABLE 2: a−b Stokes Shifts Computed Using the Semicontinuum Model

solvent	dielectric constants	orientation-dependent Stokes shifts[a] (cm^{-1})
CS_2	$\epsilon_{st} = 2.64$, $\epsilon_{op} = 2.65$	6.7
		4.3
CCl_4	$\epsilon_{st} = 2.24$, $\epsilon_{op} = 2.13$	3.4
		1.5
		1.1
Freon-113	$\epsilon_{st} = 2.41$, $\epsilon_{op} = 1.84$	14
		0.2
		15
		0.2

[a] For a given solvent, a Stokes shift is reported for each $M-O_2$ orientation considered.

Acknowledgment. This work was supported by the Danish Natural Science Research Council.

References and Notes

(1) Ogilby, P. R. *Acc. Chem. Res.* **1999**, *32*, 512−519.
(2) Schmidt, R.; Shafii, F.; Hild, M. *J. Phys. Chem. A.* **1999**, *103*, 2599−2605.
(3) Foote, C. S.; Clennan, E. L. Properties and Reactions of Singlet Dioxygen. In *Active Oxygen in Chemistry;* Foote, C. S., Valentine, J. S., Greenberg, A. and Liebman, J. F., Eds.; Chapman and Hall: London, 1995; pp 105−140.
(4) Frimer, A. A. (Ed.) *Singlet Oxygen*; CRC Press: Boca Raton, 1985; Vol I−IV.

(5) Macpherson, A. N.; Truscott, T. G.; Turner, P. H. *J. Chem. Soc., Faraday Trans.* **1994**, *90*, 1065−1072.
(6) Wessels, J. M.; Rodgers, M. A. J. *J. Phys. Chem.* **1995**, *99*, 17586−17592.
(7) Evans, D. F. *Chem. Commun.* **1969**, 367−368.
(8) Matheson, I. B. C.; Lee, J. *Chem. Phys. Lett.* **1971**, *8*, 173−176.
(9) Long, C.; Kearns, D. R. *J. Chem. Phys.* **1973**, *59*, 5729−5736.
(10) Losev, A. P.; Nichiporovich, I. N.; Byteva, I. M.; Drozdov, N. N.; Al Jghgami, I. F. *Chem. Phys. Lett.* **1991**, *181*, 45−50 (Erratum: *Chem. Phys. Lett.* **1991**, *186*, 586).
(11) Weldon, D.; Ogilby, P. R. *J. Am. Chem. Soc.* **1998**, *120*, 12978−12979.
(12) Keszthelyi, T.; Weldon, D.; Andersen, T. N.; Poulsen, T. D.; Mikkelsen, K. V.; Ogilby, P. R. *Photochem. Photobiol.* **1999**, *70*, 531−539.
(13) Chou, P.-T.; Frei, H. *Chem. Phys. Lett.* **1985**, *122*, 87−92.
(14) Weldon, D.; Wang, B.; Poulsen, T. D.; Mikkelsen, K. V.; Ogilby, P. R. *J. Phys. Chem. A* **1998**, *102*, 1498−1500.
(15) Poulsen, T. D.; Ogilby, P. R.; Mikkelsen, K. V. *J. Phys. Chem. A* **1998**, *102*, 8970−8973.
(16) Poulsen, T. D.; Ogilby, P. R.; Mikkelsen, K. V. *J. Phys. Chem. A.* **1999**, *103*, 3418−3422.
(17) Weldon, D.; Poulsen, T. D.; Mikkelsen, K. V.; Ogilby, P. R. *Photochem. Photobiol.* **1999**, *70*, 369−379.
(18) Guelachvili, G.; Rao, K. N. *Handbook of Infrared Standards II*; Academic Press: Boston, **1993**.
(19) Griffiths, P. R.; de Haseth, J. A. *Fourier Transform Infrared Spectrometry*; John Wiley and Sons: New York, 1986.
(20) Koechner, W. *Solid-State Laser Engineering*; Springer-Verlag: Berlin, 1992.
(21) Mikkelsen, K. V.; Dalgaard, E.; Swanstrøm, P. *J. Phys. Chem.* **1987**, *91*, 3081−3092.
(22) Mikkelsen, K. V.; Ågren, H.; Jensen, H. J. A.; Helgaker, T. *J. Chem. Phys.* **1988**, 89, 3086−3095.
(23) Mikkelsen, K. V.; Cesar, A.; Ågren, H.; Jensen, H. J. A. *J. Chem. Phys.* **1995**, *103*, 9010−9023.
(24) Helgaker, T.; Jensen, H. J. A.; Jørgensen, P.; Olsen, J.; Ruud, K.; Ågren, H.; Andersen, T.; Bak, K. L.; Bakken, V.; Christiansen, O.; Dahle, P.; Dalskov, E. K.; Enevoldsen, T.; Fernandez, B.; Heiberg, H.; Hettema, H.; Jonsson, D.; Kirpekar, S.; Kobayashi, R.; Koch, H.; Mikkelsen, K. V.; Norman, P.; Packer, M. J.; Saue, T.; Taylor, P. R.; Vahtras, O. Dalton, an ab initio electronic structure program, release 1.0, 1997. See http://www.kjemi.uio.no/software/dalton/dalton.html.
(25) Mikkelsen, K. V.; Jørgensen, P.; Jensen, H. J. A. *J. Chem. Phys.* **1994**, *100*, 6597−6607.
(26) Mikkelsen, K. V.; Sylvester-Hvid, K. O. *J. Phys. Chem.* **1996**, *100*, 9116−9126.
(27) Olsen, J.; Jørgensen, P. *J. Chem. Phys.* **1985**, *82*, 3235−3264.
(28) Minaev, B. F.; Ågren, H. *J. Chem. Soc., Faraday Trans.* **1997**, *93*, 2231−2239.
(29) Jensen, F. *Introduction to Computational Chemistry*; John Wiley and Sons: Chichester, 1999.
(30) Schmidt, R.; Bodesheim, M. *J. Phys. Chem. A* **1998**, *102*, 4769−4774.
(31) Marcus, R. A. *J. Phys. Chem.* **1992**, *96*, 1753−1757.
(32) Young, R. H. *J. Chem. Phys.* **1992**, *97*, 8261−8275.
(33) Kim, H. J.; Bianco, R.; Gertner, B. J.; Hynes, J. T. *J. Phys. Chem.* **1993**, *97*, 1723−1728.
(34) Jortner, J. *Mol. Phys.* **1962**, *5*, 257−270.
(35) Billing, G. D.; Mikkelsen, K. V. *Advanced Molecular Dynamics and Chemical Kinetics*; John Wiley and Sons: New York, 1997.
(36) Medina-Llanos, C.; Ågren, H.; Mikkelsen, K. V.; Jensen, H. J. A. *J. Chem. Phys.* **1989**, *90*, 6422−6435.
(37) Andersen, L. K.; Ogilby, P. R. Submitted for publication.